Novel formulation for the effects of sloshing with capillarity on elastic structures in linear dynamics

Roger Ohayon, Christian Soize, Quentin Akkaoui, Evangéline Capiez-Lernout

Novel formulation for the effects of sloshing with capillarity on elastic structures in linear dynamics

R. Ohayon[a], C. Soize[*,b], Q. Akkaoui[b], E. Capiez-Lernout[b]

[a] *Structural Mechanics and Coupled Systems Lab, Conservatoire National des Arts et Métiers, 292 rue Saint Martin, 75003 Paris, France*
[b] *Université Paris-Est Marne-la-Vallée, MSME UMR 8208 CNRS, 5 bd Descartes, 77454 Marne-La-Vallée, France*

Abstract

This paper is devoted to the linear dynamics of liquid-structure interactions for an elastic structure filled with compressible liquid (acoustic liquid), with sloshing and with capillarity effects on the free surface in presence of a gravity field. The objective is to detail the formulation and to quantify the role played by the elasticity in the neighborhood of the triple contact line between the free surface of the compressible liquid and the elastic structure in presence of sloshing and capillarity effects. Most of the works consider that the structure is totally not deformable (rigid tank). Nevertheless, for taking into account the elasticity of the tank, some works have introduced an approximation, which consists in considering a locally undeformable structure in the neighborhood of the triple contact line. The theory presented requires the use of quadratic finite elements for discretizing a new introduced boundary condition. An application has specifically been constructed and presented for quantifying the role played by the elasticity of the structure in the neighborhood of the triple contact line.

Key words: sloshing, surface tension, elastic structure, elasto-capillarity, compressible fluid, structural acoustics, boundary conditions on the triple line, linear dynamics, reduced-order model

1. Introduction

This paper is devoted to the computational quantification of the effects of sloshing with capillarity on elastic structures coupled with a liquid for linear vibrations, in which the capillarity effects are only considered at the macroscopic level. More precisely, we consider a tank that is modeled by a linear damped elastic structure filled with a linear dissipative compressible liquid (acoustic liquid) exhibiting a free surface in presence of a gravity field and surface tension (capillarity). This problem has intensively been analyzed in the literature in neglecting the capillarity effects. The sloshing is often modeled using an incompressible liquid. However, in this paper, the liquid is an acoustic fluid, that is to say, is a compressible fluid and there is no flow. This means that we are interested in the general case of an elastoacoustic (vibroacoustic) problem of an elastic structure coupled with an acoustic liquid. In addition, for this problem, the sloshing

[*]Corresponding author: C. Soize, christian.soize@u-pem.fr

Preprint of the published paper in International Journal for Numerical Methods in Engineering, 2020, doi:10.1002/nme.6290, 1-21.

and the capillarity are taken into account because these phenomena can play an important role in the vibroacoustic problem for specific dimensions of the geometry.

The linear sloshing in a rigid tank filled with an inviscid incompressible liquid without capillarity effects was analyzed, for instance, by Abramson 1966 [1], by Moiseyev and Rumyansev 1968 [2], by Morand and Ohayon 1995 [3], by Dodge 2000 [4], by Ibrahim 2005 [5], and by Faltinsen *et al* 2009 [6].

The case of the computational fluid-structure interaction of a linear elastic structure filled with a linear inviscid incompressible liquid, which allows the added-mass effects to be taken into account, was analyzed, for instance, by Chowdhury 1972 [7], by Morand and Ohayon 1995 [3], by Amabili, Paidoussis, and Lakis 1998 [8], by Zienkiewicz, Taylor, and Zhu 2005 [9] in Chapter 18, and by Farhat *et al* 2013 [10]. In this framework, the sloshing free surface effects, without including the elasto-gravity operator, can be found in Bermudez *et al* 2003 [11], in Gonzalez *et al* 2012 [12], and in Amabili *et al* 1998 [8], while taking into account the elasto-gravity operator, these effects can be found in Morand and Ohayon 1995 [3] and in Schotte and Ohayon 2005 [13].

Concerning the computational fluid-structure interaction of a linear elastic structure filled with a linear compressible liquid (acoustic liquid), without sloshing and without capillarity effects, has been analyzed by Ohayon and Soize in 1997 [14], Brummelen in 2009 [15], and by Bazilevs, Takaziwa, and Tezduyar 2013 [16]. Taking into account the effects of sloshing and internal gravity, still without capillarity effects, can be found in Lighthill 1978 [17] and in Andrianarison and Ohayon 2006 [18].

This paper is specifically devoted to the fluid-structure interaction of a linear elastic structure filled with a linear compressible liquid (acoustic liquid), with sloshing and with capillarity effects on the free surface in presence of a gravity field, still neglecting the elasto-gravity operator and the internal gravity effects, which are assumed to be of second order with respect to the phenomena taken into account. Because the objective is to detail the formulation and to quantify the role played by the contact line between the free surface of the compressible liquid and the elastic structure in presence of sloshing and capillarity effects, the developments are restricted to the linear case, because the introduction of nonlinearities does not change the analysis and the nature of the difficulties induced by the contact line. The case of linear elastic structure coupled with a nonlinear incompressible fluid can be found in Chu and Kana 1967 [19] and in Dias and Kharif 1999 [20], while the case of a nonlinear elastic structure with a linear compressible fluid can be found in Ohayon and Soize 2016 [21] and in Akkaoui *et al* 2019 [22] that reinterprets the experimental studies performed by Abramson *et al* 1966 [23] and 1970 [24].

Before positioning the novelty of this work related to the taking into account of the effects of the capillarity, for general physics aspects, we refer the reader to [25, 26, 27, 28]. Concerning the classical macroscopic equations for capillarity in which the surface-tension coefficient is assumed to be constant with respect to the spatial coordinates, we refer the reader to [29, 27]. For models based on the use of the incompressible Navier-Stokes equations with a classical surface-tension equation, see [30, 31, 32, 33, 34, 35, 36] and a more refined model based on the Cahn-Hilliard Navier-Stokes equations can be found in [37]. For non-constant surface-tension coefficient, we refer the reader to [38, 39, 40]. For the capillarity modeling at the macroscopic level, the contact line is located at the intersection of free surface of the liquid and the structure. The contact angle between the free surface of the liquid and the elastic wall of the structure is a direct consequence of the molecular interactions among the structural and liquid materials

at the contact line. This important parameter controls the geometry of the free surface in the neighborhood of the contact line. In the classical capillarity theory, the contact angle is constant [41, 42, 27]. Let us note that there are many works related to the analysis of the contact angle (i) using a detailed spatial structure of the capillary forces [43], (ii) considering a non-constant angle and moving contact line in statics and dynamics [44, 45, 46, 47, 48], (iii) using local formulation at the microscopic and molecular dynamics levels [49, 50, 51, 52].

We are interested in developing a computational model of a linear damped elastic structure partially filled with a linear dissipative acoustic liquid exhibiting a free surface with sloshing and capillarity. The novelty of this paper is to present an appropriate force-type boundary condition on the contact line for a deformable elastic structure. A numerical validation will quantify its effects with respect to the classical approximation consisting in considering that the structure is not deformable in the neighborhood of the contact line. Most of the works consider that the structure is totally not deformable (rigid tank) [53, 54, 55, 56, 57]. Nevertheless, for taking into account the elasticity of the tank, some works have introduced a nonphysical approximation, which consists in considering a locally undeformable structure in the neighborhood of the contact line. The boundary value problem of the coupled system involving the force-type boundary condition on the contact line for a deformable elastic structure has been presented in[58]. In this paper, this boundary value problem is detailed and its weak formulation is presented for constructing the finite element approximation. The weak formulation will show that the finite elements for the discretization of the coupled problem must be quadratic and not linear as it is usually done when the tank is assumed to be not elastic or when the structure is assumed to be elastic but without capillarity. An appropriate coupled system has been constructed in order to clearly quantifying the effects of this new term that appears in the structure equations.

The outline of the paper is the following. The definition of the fluid-structure coupled system is presented in Section 2 and the formulation for the liquid with sloshing and capillarity in the case of a prescribed boundary displacement is presented in Section 3. Section 4 deals with the coupling boundary condition for the elastic structure on the fluid-structure interface and Section 5 is devoted to the formulation for the elastic structure coupled with the liquid with sloshing and capillarity in which the new boundary condition defined in Scetion 4 is introduced. In Section 7, we present an application that has specifically been designed for quantifying the role played by the elasticity of the structure in the neighborhood of the triple line. The paper finishes with a conclusion and a reference sections.

2. Definition of the fluid-structure coupled system

The physical space is referred to a cartesian reference system $(\mathbf{e}_1, \mathbf{e}_2, \mathbf{e}_3)$ for which the generic point is denoted by $\mathbf{x} = (x_1, x_2, x_3)$. The reference configuration of the considered fluid-structure system is defined in Figure 1. The undeformed structure (natural state) occupies an open, bounded, and connected subset Ω_S of $\mathbb{R}^3$. It contains a liquid that occupies an open and bounded domain Ω_L (the geometry of domain Ω_L results from a pre-computation for finding the static equilibrium of the free surface of the liquid). Let γ be the contact line of the free surface with the structure. The free surface is represented by the open subset Γ. The boundary of Ω_L is the closed set $\partial\Omega_L = \Gamma \cup \gamma \cup \Gamma_L$ in which Γ_L is an open subset. The boundary of Ω_S is the set $\partial\Omega_S = \Gamma_E \cup \Sigma$ in which Γ_E is a closed subset representing the external boundary of the structure

while Σ is defined by

$$\Sigma = \Gamma_L \cup \gamma \cup \Gamma_G \quad \text{with} \quad \Gamma_L \cap \gamma = \emptyset \quad , \quad \gamma \cap \Gamma_G = \emptyset \quad , \quad \Gamma_L \cap \Gamma_G = \emptyset \,, \tag{1}$$

is a closed subset representing the internal boundary in which Γ_G is an open part of the internal boundary that is not in contact with the liquid. The boundary of the open parts Γ_L and Γ_G is the curve γ. It is assumed that surfaces Γ, Γ_L, Γ_G, Σ, and line γ are smooth. The domain whose boundary is the closed set $\Gamma \cup \gamma \cup \Gamma_G$ is empty or is filled by a gas whose effects are neglected for sake of brevity. The unit normal to $\partial\Omega_S$ external to Ω_S is denoted as $\mathbf{n}^S$ while the one to $\partial\Omega_L$ external to Ω_L is denoted as $\mathbf{n}$. On the common interface Γ_L, we have $\mathbf{n}^S = -\mathbf{n}$. The unit normal to γ external to Γ, which belongs to the tangent plane to surface Γ at line γ, is denoted as $\boldsymbol{\nu}$. Similarly, the unit normal to γ external to Γ, which belongs to the tangent plane to surface Γ_L at line γ, is denoted as $\boldsymbol{\nu}_L$.

At time t, the structure is described by its displacement field $\mathbf{x} \mapsto \mathbf{u}(\mathbf{x}, t) = (u_1(\mathbf{x}, t), u_2(\mathbf{x}, t), u_3(\mathbf{x}, t))$

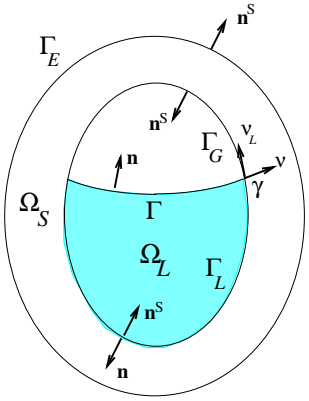

Figure 1: Geometry of the coupled system.

for $\mathbf{x} \in \Omega_S$. The constitutive equation for the structure is assumed to be linear viscoelastic with instantaneous memory. The liquid is modeled by a linear dissipative acoustic fluid that is assumed to be homogeneous, compressible, inviscid with a volumetric additional dissipative term. Its infinitesimal motions with respect to the reference configuration are irrotational. At time t, it is described by a pressure field $\mathbf{x} \mapsto p(\mathbf{x}, t)$ for $\mathbf{x} \in \Omega_L$. It should be noted that the liquid is assumed to be inviscid on the fluid-structure interface on which a slip condition will be written [14, 59]. At time t, the normal displacement of the free surface is described by the field $\mathbf{x} \mapsto h(\mathbf{x}, t)$ for $\mathbf{x} \in \Gamma$.

We are interested in analyzing the linear dynamics of the coupled system around its reference configuration. Since the structure of the coupled system is not subjected to zero Dirichlet conditions (thus there are possible rigid body displacements), it is assumed that, at each time, the work of the external forces in the rigid body displacements is zero. At time t, in the reference configuration, the boundary value problem of the coupled system will be expressed in terms of the structural displacement field $\mathbf{u}(\cdot, t)$, the internal pressure field $p(\cdot, t)$, and the normal displacement $h(\cdot, t)$ of the free surface.

Before introducing the boundary value problem relative to the coupled system under consideration for which the liquid is coupled with an elastic structure on the interface Γ_L in presence of capillarity, we first detail the particular case of the liquid occupying Ω_L, with the free surface Γ, and for which a given displacement field $\mathbf{u}$ is imposed to interface Γ_L. The introduction of such a boundary value problem allows for summarizing the classical part of the formulation. In Section 5, we will take into account the coupling with the elastic structure, which requires additional developments in order to take into account the actions of the liquid on the elastic structure on line γ, because the structural surface forces have to be balanced with line forces induced by the capillarity.

3. Formulation for the liquid with sloshing and capillarity in the case of a prescribed boundary displacement

3.1. Boundary value problem

For the linear dissipative acoustic liquid occupying Ω_L, the equation of motion is the wave equation with an additional dissipative term expressed in term of the acoustic pressure field p. For the free surface Γ, the equation of motion is a linearized dynamic equation expressed in term of the displacement h of the free surface measured along the normal $\mathbf{n}$ to Γ, external to Ω_L.

For a given displacement field, $\mathbf{x} \mapsto \mathbf{u}_\Sigma(\mathbf{x}, t)$ on Γ_L with values in $\mathbb{R}^3$, and for given Cauchy initial conditions at $t = 0$, we have to solve the following boundary value problem consisting in finding the fields $\{p(\cdot, t), t > 0\}$ and $\{h(\cdot, t), t > 0\}$ such that

$$\frac{1}{\rho_0 c_0^2}\frac{\partial^2 p}{\partial t^2} - \frac{\tau}{\rho_0}\boldsymbol{\nabla}^2\frac{\partial p}{\partial t} - \frac{1}{\rho_0}\boldsymbol{\nabla}^2 p = 0 \quad \text{in} \quad \Omega_L\,, \tag{2}$$

$$(1 + \tau\frac{\partial}{\partial t})\frac{\partial p}{\partial \mathbf{n}} = -\rho_0\frac{\partial^2 \mathbf{u}_\Sigma}{\partial t^2}\cdot\mathbf{n} \quad \text{on} \quad \Gamma_L\,, \tag{3}$$

$$(1 + \tau\frac{\partial}{\partial t})\frac{\partial p}{\partial \mathbf{n}} = -\rho_0\frac{\partial^2 h}{\partial t^2} \quad \text{on} \quad \Gamma\,, \tag{4}$$

$$p = \rho_0\, h\, \mathbf{g}\cdot\mathbf{n} - \sigma_\Gamma\{(\frac{1}{R_1^2} + \frac{1}{R_2^2})h + \boldsymbol{\nabla}_\Gamma^2 h\} \quad \text{on} \quad \Gamma\,, \tag{5}$$

$$\frac{\partial h}{\partial \boldsymbol{\nu}} = c_h\, h + \mathcal{J}\mathbf{u}_\Sigma \quad \text{on} \quad \gamma\,, \tag{6}$$

with the following definition of the linear operator $\mathcal{J}$,

$$\mathcal{J}\mathbf{u}_\Sigma = -d_h\,\mathbf{u}_\Sigma\cdot\mathbf{n} + \frac{\partial(\mathbf{u}_\Sigma\cdot\mathbf{n})}{\partial \boldsymbol{\nu}_L} \quad \text{on} \quad \gamma\,. \tag{7}$$

- Equation (2) is the wave equation with a dissipative term, in which ρ_0 is the constant mass density of the homogeneous liquid at equilibrium, c_0 the corresponding constant speed of sound, and the constant coefficient τ characterizes the dissipation in the liquid [14, 59].

- Equation (3) is the kinematic fluid-structure coupling condition on Γ_L, which expresses the continuity of the normal acceleration field on the interface [14, 59].

- Equation (4) is the kinematic equation expressed in term of the displacement h of the free surface measured along the normal $\mathbf{n}$ to Γ [14, 59].

- Equation (5) corresponds to the free-surface constitutive equation of surface Γ, in which σ_Γ is the constant surface tension coefficient, $\mathbf{g}$ is the gravitational acceleration vector, R_1 and R_2 are the principal curvature radii, and where $\boldsymbol{\nabla}^2_\Gamma h$ denotes the surface Laplacian related to surface Γ. The term $(1/R_1^2 + 1/R_2^2)\, h + \boldsymbol{\nabla}^2_\Gamma h$ results from the change of the surface energy induced by an infinitesimal change in h, which yields a contribution to the surface pressure (classical Young-Laplace law) [27, 2, 3].

- In Equations. (6) and (7), the first term in the right-hand side corresponds to the classical contact angle condition on γ in which c_h is the contact angle coefficient. The second term is an additional term that allows the given displacement field, $\mathbf{x} \mapsto \mathbf{u}_\Sigma(\mathbf{x}, t)$ on Γ_L to be taken into account. In this term, at a given point in line γ, d_h is a real coefficient depending on the mean curvature $< K_\Gamma >$ of surface Γ and on the mean curvature $< K_\Sigma >$ of surface $\Sigma = \Gamma_L \cup \gamma \cup \Gamma_G$. The coefficients d_h and c_h are defined by

$$d_h = \frac{< K_\Gamma > - < K_\Sigma > \cos(\theta)}{\sin(\theta)} \quad , \quad c_h = \frac{< K_\Gamma > \cos(\theta) - < K_\Sigma >}{\sin(\theta)} \,, \tag{8}$$

  in which θ is the contact angle that is independent of time t. For details concerning the derivation of $\mathcal{J}$, we refer the reader to [3] in which the present boundary value problem has been treated considering an inviscid and incompressible liquid using the displacement potential field instead of the pressure field p. It should be noted that, if $\mathbf{u}_\Sigma = 0$ on Σ, then the classical boundary condition on γ is obtained. If $\mathbf{u}_\Sigma$ corresponds to a rigid body motion (6 degrees of freedom), then the boundary condition is written as $\mathcal{J}\mathbf{u}_\Sigma = -d_h\, \mathbf{u}_\Sigma \cdot \mathbf{n}$.

3.2. Weak formulation

Following Section 3.1, field $\mathbf{u}_\Sigma$ is prescribed. For constructing the weak formulation of the boundary value problem defined by Eqs. (2) to (7), we introduce the following admissible spaces for test functions, $\mathbf{x} \mapsto \delta p(\mathbf{x})$, concerning the pressure field p defined in Ω_L and for test functions, $\mathbf{x} \mapsto \delta h(\mathbf{x})$, the normal displacement h of the free surface defined on Γ,

$$C_p := H^1(\Omega_L, \mathbb{R}) = \{\delta p \in L^2(\Omega_L)\,,\ \frac{\partial \delta p}{\partial x_j} \in L^2(\Omega_L)\,,\ j = 1, 2, 3\}\,, \tag{9}$$

$$C_h := H^1(\Gamma, \mathbb{R}) = \{\delta h \in L^2(\Gamma)\,,\ \frac{\partial \delta h}{\partial x_j} \in L^2(\Gamma)\,,\ j = 1, 2, 3\}\,. \tag{10}$$

The weak formulation of Eq. (2) with the boundary conditions defined by Eqs. (3) and (4) is written, for all δp in C_p, as

$$\frac{1}{\rho_0 c_0^2} \int_{\Omega_L} \frac{\partial^2 p}{\partial t^2}\, \delta p \, d\mathbf{x} + \frac{\tau}{\rho_0} \int_{\Omega_L} \boldsymbol{\nabla} \frac{\partial p}{\partial t} \cdot \boldsymbol{\nabla} \delta p \, d\mathbf{x} + \frac{1}{\rho_0} \int_{\Omega_L} \boldsymbol{\nabla} p \cdot \boldsymbol{\nabla}\, \delta p \, d\mathbf{x} + \int_\Gamma \frac{\partial^2 h}{\partial t^2}\, \delta p \, ds_\Gamma$$
$$= - \int_{\Gamma_L} \frac{\partial^2 \mathbf{u}_\Sigma}{\partial t^2} \cdot \mathbf{n}\ \delta p \, ds_{\Gamma_L}\,. \tag{11}$$

The weak formulation of Eq. (5) with the boundary condition defined by Eq. (6) with Eq. (7) is written, for all δh in C_h, as

$$-\int_\Gamma p\,\delta h\,ds_\Gamma + \rho_0\int_\Gamma \mathbf{g}\cdot\mathbf{n}\,h\,ds_\Gamma + k_c(h,\delta h) = \sigma_\Gamma\int_\gamma (\mathcal{J}\mathbf{u}_\Sigma)\,\delta h\,ds_\gamma\,, \tag{12}$$

in which $k_c(h,\delta h)$ is the bilinear form defined by

$$k_c(h,\delta h) = \sigma_\Gamma\int_\Gamma \boldsymbol{\nabla}_\Gamma h\cdot\boldsymbol{\nabla}_\Gamma\delta h\,ds_\Gamma - \sigma_\Gamma\int_\Gamma (\frac{1}{R_1^2}+\frac{1}{R_2^2})\,h\,\delta h\,ds_\Gamma - \sigma_\Gamma\int_\gamma c_h h\,\delta h\,ds_\gamma\,. \tag{13}$$

4. Coupling boundary condition for the elastic structure on the fluid-structure interface

The displacement field of the structure is the field $\mathbf{u}(\cdot,t)$ defined on Ω_S for which its trace on Σ is denoted by $\mathbf{u}_\Sigma(\cdot,t)$. Let $\sigma = \{\sigma_{ij}\}_{1\le i,j\le 3}$ be the tensor-valued stress field defined in Ω_S. It is assumed that there are no external forces on Γ_G

$$\sigma\,\mathbf{n}^S = \mathbf{0} \quad \text{on} \quad \Gamma_G\,. \tag{14}$$

The coupling boundary condition for the elastic structure on the fluid-structure interface consists in expressing the field $\sigma\,\mathbf{n}^S$ on boundary Γ_L as a function of p and h. Classically, without capillarity effects, this boundary condition is written as

$$\sigma\,\mathbf{n}^S = p\,\mathbf{n} \quad \text{on} \quad \Gamma_L\,. \tag{15}$$

As pointed out in [3], the modeling of the coupling boundary condition of the 3D elastic medium in terms of $\sigma\mathbf{n}^S$ per unit area on Σ, at the contact line γ of the free surface Γ, remains an open problem unresolved to date. Indeed, the capillarity model used introduces a linear density of surface-tension forces on γ that cannot be balanced by the $\sigma\,\mathbf{n}^S$ surface density of structural forces on Σ. In this section, we thoroughly detail an appropriate formulation that has been sketched in [58] and which is consistent with Eq. (6). In this section, for simplifying the notation, time t is omitted, and for the mathematical results used concerning the Sobolev spaces (integer and fractional orders), we refer the reader to [60].

The first step of the construction consists in introducing a functional analysis framework for interpreting Eqs. (6) and (7) and for defining operator $\mathcal{J}$.

- Let us assume that displacement field $\mathbf{u} = (u_1, u_2, u_3)$ belongs to Sobolev space $H^2(\Omega_S, \mathbb{R}^3)$. Consequently, its trace $\mathbf{u}_\Sigma$ on Σ belongs to Sobolev space $H^{3/2}(\Sigma, \mathbb{R}^3)$. It should be noted that the continuous injection from $H^2(\Omega_S, \mathbb{R}^3)$ into $C^0(\overline{\Omega}_S, \mathbb{R}^3)$ is compact.

- Let us assume that the normal displacement field h belongs to Sobolev space $H^1(\Gamma, \mathbb{R})$. Therefore, its trace h_γ on γ belongs to Sobolev space $H^{1/2}(\gamma, \mathbb{R})$. Under those assumptions, $\mathcal{J}$ appearing in Eq. (6), is a linear operator from $H^{3/2}(\Sigma, \mathbb{R}^3)$ into the Hilbert space $L^2(\gamma, \mathbb{R})$ that is a subspace of $H^{-1/2}(\gamma, \mathbb{R})$. In order to define the weak formulation of Eq. (6), we introduce the duality bracket $< h, \mathcal{J}\mathbf{u}_\Sigma >_\gamma$ between h in $H^{1/2}(\gamma, \mathbb{R})$ and $\mathcal{J}\mathbf{u}_\Sigma$ in $H^{-1/2}(\gamma, \mathbb{R})$. It should be noted that, for h_γ and $\mathcal{J}\mathbf{u}_\Sigma$ in $L^2(\gamma, \mathbb{R})$, the duality bracket coincides with the Hilbert inner product in $L^2(\gamma, \mathbb{R})$, that is to say,

$$< h, \mathcal{J}\mathbf{u}_\Sigma >_\gamma = \int_\gamma h(\mathbf{x})\,(\mathcal{J}\mathbf{u}_\Sigma)(\mathbf{x})\,ds_\gamma(\mathbf{x})\,, \tag{16}$$

  in which $\int_\gamma ds_\gamma(\mathbf{x}) = |\gamma|$ is the measure of γ.

In the second step of the construction, since the linear density of surface-tension forces on γ cannot be balanced by the $\sigma\,\mathbf{n}^S$ surface density of forces on Σ, we define this linear density of surface-tension forces on γ as a generalized function associated with the transpose operator $\mathcal{J}'$ of $\mathcal{J}$ defined using the dual bracket $< \cdot, \cdot >_\gamma$, that is to say,

$$\ll \mathcal{J}'h\,,\mathbf{u}_\Sigma \gg_\Sigma = < h, \mathcal{J}\mathbf{u}_\Sigma >_\gamma\,, \tag{17}$$

in which $\ll \cdot, \cdot \gg_\Sigma$ is the duality bracket between Sobolev space $H^{-3/2}(\Sigma, \mathbb{R}^3)$ and $H^{3/2}(\Sigma, \mathbb{R}^3)$, which shows that the transpose $\mathcal{J}'$ is a linear operator from $H^{1/2}(\gamma, \mathbb{R})$ into $H^{-3/2}(\Sigma, \mathbb{R}^3)$. Consequently, $\mathcal{J}'h$ is a generalized function whose support is γ, knowing that [61, 62] the Dirac generalized function δ_0 on manifold Σ belongs to $H^{-3/2}(\Sigma, \mathbb{R})$ and that the Sobolev injection theorem [60] allows for writing $H^{3/2}(\Sigma, \mathbb{R}^3) \subset C^0(\Sigma)$ with continuous injection.

The last step consists in writing the coupling boundary condition for the elastic structure on the fluid-structure interface Σ. Let $\mathbf{x} \mapsto \mathbb{1}_{\Gamma_L}(\mathbf{x})$ be the indicator function defined on Σ such that $\mathbb{1}_{\Gamma_L}(\mathbf{x}) = 0$ if $\mathbf{x} \notin \Gamma_L$ and $\mathbb{1}_{\Gamma_L}(\mathbf{x}) = 1$ if $\mathbf{x} \in \Gamma_L$. Let us assume that pressure field p belongs to Sobolev space $H^1(\Omega_L, \mathbb{R})$. Therefore the trace p_{Γ_L} of p on the part Γ_L of $\partial\Omega_L$ belongs to Sobolev space $H^{1/2}(\Gamma_L, \mathbb{R})$. We introduce the function $\mathbf{x} \mapsto \mathbb{1}_{\Gamma_L}(\mathbf{x})\, p_{\Gamma_L}(\mathbf{x})$ that belongs to Sobolev space $H^{1/2}(\Sigma, \mathbb{R})$. Consequently, taking into account Eq. (14), the appropriate boundary condition on interface Σ is written as

$$(\sigma\,\mathbf{n}^S)(\mathbf{x})\,ds_\Sigma(\mathbf{x}) = \mathbb{1}_{\Gamma_L}(\mathbf{x})\,p_{\Gamma_L}(\mathbf{x})\,\mathbf{n}(\mathbf{x})\,ds_\Sigma(\mathbf{x}) + \sigma_\Gamma\,(\mathcal{J}'h)(\mathbf{x}) \quad \text{on} \quad \Sigma\,, \tag{18}$$

that has to be read in the sense of an equality of generalized functions. Concerning the first term in the right-hand-side of Eq. (18), since $\mathbf{x} \mapsto f(\mathbf{x}) = \mathbb{1}_{\Gamma_L}(\mathbf{x})\,p_{\Gamma_L}(\mathbf{x})$ is a locally integrable function on Σ, the measure $f(\mathbf{x})\,ds_\Sigma(\mathbf{x})$ on Σ defined a generalized function F such that for all infinitely differentiable function φ on Σ, $\ll F, \varphi \gg_\Sigma = \int_\Sigma f(\mathbf{x})\,\varphi(\mathbf{x})\,ds_\Sigma(\mathbf{x})$ in which $F = f\,ds_\Sigma$.

5. Formulation for the elastic structure coupled with the liquid with sloshing and capillarity

The coupled fluid-structure system is constituted of the equations of the boundary value problem in (p, h), defined in Section 3.1, in which the trace $\mathbf{u}_\Sigma$ on Σ of the displacement field $\mathbf{u}$ is now an unknown. To these equations, those for the elastic structure have to be added. We are interested in studying the linear dynamics of the fluid-structure system around a stable static equilibrium, which is considered as a natural state at rest (the external structural forces are assumed to be in equilibrium).

5.1. Boundary value problem for the elastic structure

The structure in constituted of a heterogeneous linear viscoelastic material with instantaneous memory for which the constitutive equation is written (see Chapter 4, Section3 in [14]) as

$$\sigma_{ij} = a_{ijkh}(\mathbf{x})\,\varepsilon_{kh}(\mathbf{u}) + b_{ijkh}(\mathbf{x})\,\varepsilon_{kh}(\partial\mathbf{u}/\partial t)\,, \tag{19}$$

in which ε is the linear strain tensor such that $\varepsilon_{kh}(\mathbf{u}) = (\partial u_k/\partial x_h + \partial u_h/\partial x_k)/2$. The structure is subjected to a body force field $\mathbf{x} \mapsto \mathbf{f}^{\text{vol}}(\mathbf{x}, t)$ defined on Ω_s, to a surface force field $\mathbf{x} \mapsto \mathbf{f}^{\text{surf}}(\mathbf{x}, t)$ defined on Γ_E, and to the pressure field of the liquid. The equations for the elastic structure,

formulated in terms of displacement field $\mathbf{u}$, with its boundary equations for which Eq. 18 is used, are written as

$$\rho_S \frac{\partial^2 \mathbf{u}}{\partial t^2} - \operatorname{div} \sigma = \mathbf{f}^{\text{vol}} \ , \ \forall \mathbf{x} \in \Omega_S \ , \tag{20}$$

$$\sigma \, \mathbf{n}^S = \mathbf{f}^{\text{surf}} \quad \text{on} \quad \Gamma_E \, , \tag{21}$$

$$\sigma \, \mathbf{n}^S = \mathbf{0} \quad \text{on} \quad \Gamma_G \, , \tag{22}$$

$$\sigma \, \mathbf{n}^S = \mathbb{1}_{\Gamma_L} \, p \, \mathbf{n} + \sigma_\Gamma \, \mathcal{J}' h \quad \text{on} \quad \Sigma \, , \tag{23}$$

It should be noted that Eqs. (20) to (23) will be used in the next subsection for writing the associated weak formulation in which Eq. (23) will be interpreted in the framework of the theory of generalized functions.

5.2. Weak formulation for the elastic structure coupled with the liquid with sloshing and capillarity

For constructing the weak formulation of the boundary value problem related to the fluid-structure coupled system, in addition to the two admissible sets C_p and C_h defined by Eqs. (9) and (10), the admissible set $C_{\mathbf{u}}$ of test functions, $\mathbf{x} \mapsto \delta\mathbf{u}(\mathbf{x})$, has to be defined for the displacement field of the structure modeled in the 3D elasticity theory. In the classical weak formulation, if there was no capillarity effects, then $C_{\mathbf{u}}$ would be chosen as $H^1(\Omega_s, \mathbb{R}^3)$. Since there is the capillarity effects, as shown in Section 4, it should be noted that the admissible set $C_{\mathbf{u}}$ has to be chosen as $H^2(\Omega_s, \mathbb{R}^3)$, that is to say,

$$C_{\mathbf{u}} = \{\delta\mathbf{u} \in L^2(\Omega_S, \mathbb{R}^3) \, , \, \frac{\partial \delta\mathbf{u}}{\partial x_j} \in L^2(\Omega_S, \mathbb{R}^3) \, , \, \frac{\partial^2 \delta\mathbf{u}}{\partial x_j \partial x_k} \in L^2(\Omega_S, \mathbb{R}^3) \, , \text{ for } j \text{ and } k = 1, 2, 3\} \, . \tag{24}$$

It can be noted right now that this will require the choice of finite elements that are quadratic and not linear. The weak formulation of Eqs. (20) to (23) is written, for all $\delta\mathbf{u}$ in $C_{\mathbf{u}}$, as

$$\begin{aligned} \int_{\Omega_S} \rho_S \frac{\partial^2 \mathbf{u}}{\partial t^2} \cdot \delta\mathbf{u} \, d\mathbf{x} + \int_{\Omega_S} b_{ijkh} \, \varepsilon_{kh}(\frac{\partial \mathbf{u}}{\partial t}) \, \varepsilon_{ij}(\delta\mathbf{u}) \, d\mathbf{x} + \int_{\Omega_S} a_{ijkh} \, \varepsilon_{kh}(\mathbf{u}) \, \varepsilon_{ij}(\delta\mathbf{u}) \, d\mathbf{x} \\ - \int_{\Gamma_L} p \, \mathbf{n} \cdot \delta\mathbf{u} \, ds_{\Gamma_L} - \sigma_\Gamma \ll \mathcal{J}' h, \delta\mathbf{u} \gg_\Sigma = \int_{\Omega_S} \mathbf{f}^{\text{vol}} \cdot \delta\mathbf{u} \, d\mathbf{x} + \int_{\Gamma_E} \mathbf{f}^{\text{surf}} \cdot \delta\mathbf{u} \, ds_{\Gamma_E} \, . \end{aligned} \tag{25}$$

The weak formulation of the elastic structure coupled with the liquid with sloshing and capillarity is then given, for all δp in C_p, for all δh in C_h, and for all $\delta\mathbf{u}$ in $C_{\mathbf{u}}$, by Eqs. (11), (12), and (25). We recall that $\mathbf{u}_\Sigma$ is the trace of $\mathbf{u}$ on Σ.

5.3. Finite element approximation for the coupled system

As explained in Section (5.2), quadratic-interpolation finite elements have to be used for constructing the computational model, which will be the case for the application presented in Section 7.

5.3.1. Matrices of the discretized problem

Matrices related to the equations for the compressible liquid (weakly dissipative).

- Let $[M]$ be the positive-definite symmetric real matrix, which is related to the discretization of $(1/\rho_0 c_0^2) \int_{\Omega_L} (\partial^2 p/\partial t^2)\, \delta p \, d\mathbf{x}$.
- Let $[D] = \tau\,[K]$ be the positive-semidefinite symmetric real matrix with a kernel of dimension 1, which is related to the discretization of $(\tau/\rho_0) \int_{\Omega_L} \boldsymbol{\nabla}(\partial p/\partial t) \cdot \boldsymbol{\nabla}\delta p \, d\mathbf{x}$.
- Let $[K]$ be the positive-semidefinite symmetric real matrix with a kernel of dimension 1, which is related to the discretization of $(1/\rho_0) \int_{\Omega_L} \boldsymbol{\nabla} p \cdot \boldsymbol{\nabla}\delta p \, d\mathbf{x}$.

Matrices related to the equations for the liquid free surface.

- Let $[K_g]$ be the positive-definite symmetric real matrix, which is related to the discretization of $\rho_0 \int_\Gamma \mathbf{g} \cdot \mathbf{n}\, h\, \delta h \, ds_\Gamma$.
- Let $[K_c]$ be the positive-definite symmetric real matrix, which corresponds to the discretization of the bilinear form $k_c(h, \delta h)$ defined by Eq. 13. The positive definiteness holds due to the linear dynamics regime around a stable static equilibrium that is considered as a natural state at rest [2, 3].

Matrices related to the equations for the elastic structure.

- Let $[M^S]$ be the positive-definite symmetric real matrix, which is related to the discretization of $\int_{\Omega_S} \rho_S\, (\partial^2 \mathbf{u}/\partial t^2) \cdot \delta\mathbf{u} \, d\mathbf{x}$.
- Let $[D^S]$ be the positive-semidefinite symmetric real matrix with a kernel of dimension 6, which is related to the discretization of $\int_{\Omega_S} b_{ijkh}\, \varepsilon_{kh}(\partial\mathbf{u}/\partial t)\, \varepsilon_{ij}(\delta\mathbf{u})\, d\mathbf{x}$.
- Let $[K^S]$ be the positive-semidefinite symmetric real matrix with a kernel of dimension 6, which is related to the discretization of $\int_{\Omega_S} a_{ijkh}\, \varepsilon_{kh}(\mathbf{u})\, \varepsilon_{ij}(\delta\mathbf{u})\, d\mathbf{x}$.

Matrices related to the coupling terms.

- Let $[C_{ph}]^T$ be the rectangular real matrix, which is related to the discretization of $-\int_\Gamma (\partial^2 h/\partial t^2)\, \delta p \, ds_\Gamma$.
- Let $[C_{p\mathbf{u}}]^T$ be the rectangular real matrix, which is related to the discretization of $-\int_{\Gamma_L} (\partial^2 \mathbf{u}_\Sigma/\partial t^2) \cdot \mathbf{n}\ \delta p \, ds_{\Gamma_L}$.
- Let $[C_{h\mathbf{u}}]$ be the rectangular real matrix, which is related to the discretization of $-\sigma_\Gamma \int_\gamma (\mathcal{J}\mathbf{u}_\Sigma)\, \delta h \, ds_\gamma$.

Vector of external forces.

- Let $F^S(t)$ be the real vector of the external forces, which is related to the discretization of $\int_{\Omega_S} \mathbf{f}^{\text{vol}} \cdot \delta\mathbf{u} \, d\mathbf{x} + \int_{\Gamma_E} \mathbf{f}^{\text{surf}} \cdot \delta\mathbf{u} \, ds_{\Gamma_E}$.

5.3.2. Computational model of the coupled system

Let $\mathbf{P}(t)$, $\mathbf{H}(t)$, and $\mathbf{U}(t)$ be the vectors corresponding to the spatial discretization of fields $p(.,t)$, $h(.,t)$, and $\mathbf{u}(.,t)$. The first-time derivative is denoted by a dot and the second-time derivative by a double dot. Using the matrices introduced in Section 5.3.1, the finite element discretization of Eqs. (11), (12), and (25) yields, for $t > 0$,

$$[M]\,\ddot{\mathbf{P}}(t) + [D]\,\dot{\mathbf{P}}(t) + [K]\,\mathbf{P}(t) - [C_{ph}]^T\,\ddot{\mathbf{H}}(t) - [C_{p\mathbf{u}}]^T\,\ddot{\mathbf{U}}(t) = \mathbf{0}\,, \tag{26}$$

$$[C_{ph}]\,\mathbf{P}(t) + ([K_g] + [K_c])\,\mathbf{H}(t) + [C_{h\mathbf{u}}]\,\mathbf{U}(t) = \mathbf{0}\,, \tag{27}$$

$$[M^S]\,\ddot{\mathbf{U}}(t) + [D^S]\,\dot{\mathbf{U}}(t) + [K^S]\,\mathbf{U}(t) + [C_{p\mathbf{u}}]\,\mathbf{P}(t) + [C_{h\mathbf{u}}]^T\mathbf{H}(t) = \mathbf{F}^S(t)\,. \tag{28}$$

It can be proved that, the problem defined by Eqs. (26) to (28) with given initial conditions at $t = 0$, has a unique solution $\{(\mathbf{P}(t), \mathbf{H}(t), \mathbf{U}(t)), t \geq 0\}$. In order to prepare the construction of the reduced-order computational model, Eqs. (26) to (28) are rewritten in a global form as

$$[A_{\text{FSI}}]\,\mathbf{X}(t) = \mathbf{F}(t)\,, \tag{29}$$

in which $\mathbf{X}(t) = (\mathbf{P}(t), \mathbf{H}(t), \mathbf{U}(t))$ and where $[A_{\text{FSI}}]$ is the matrix-valued second-order differential operator,

$$[A_{\text{FSI}}] = [M_{\text{FSI}}]\,\frac{d^2}{dt^2} + [D_{\text{FSI}}]\,\frac{d}{dt} + [K_{\text{FSI}}]\,. \tag{30}$$

5.4. Reduced-order computational model for the coupled system

We consider the weak formulation of the elastic structure coupled with the liquid with sloshing and capillarity as described in Section 5.2 and that is recalled here. For all δp in C_p, for all δh in C_h, and for all $\delta\mathbf{u}$ in $C_{\mathbf{u}}$, the weak formulation is defined by Eqs. (11) and (12) in which $\mathbf{u}_\Sigma$ (as the trace of $\mathbf{u}$ on Σ) is not prescribed (such was the case in Section 3), and by Eq. (25). The finite element discretization of this weak formulation is given by Eqs. (26), (27), and (28). It has been shown in [58], that the corresponding admissible space $C_{P,H,U}$ of the vector-valued test functions $(\delta\mathbf{P}, \delta\mathbf{H}, \delta\mathbf{U})$ can be decomposed into the following direct sum,

$$C_{P,H,U} = C_P \oplus C_H \oplus C_U\,, \tag{31}$$

in which the three vector spaces, C_P, C_H, and C_U, are defined as follows, and where, for each one, we recall how it can be spanned by solving an appropriate spectral problem.

- C_P is the admissible space of test functions $\delta\mathbf{P}$, related to the inviscid compressible liquid occupying domain Ω_L, with the boundary condition $\partial p/\partial\mathbf{n} = 0$ on Γ_L (corresponding to a fixed wall $\mathbf{u} = 0$) and $p = 0$ on Γ. We consider the subspace of C_P spanned by the acoustic modes associated with the first N_p smallest acoustical eigenfrequencies and represented by the matrix $[\mathcal{P}]$ whose the columns are the N_p acoustic modes.

- C_H is the admissible space of test functions $\delta\mathbf{H}$, related to the inviscid incompressible liquid occupying domain Ω_L, with sloshing and capillarity effects, and with the boundary condition $\partial p/\partial\mathbf{n} = 0$ on Γ_L (corresponding to a fixed wall $\mathbf{u} = 0$). We consider the subspace of C_H spanned by the sloshing-capillarity modes associated with the first N_h smallest sloshing-capillarity eigenfrequencies and represented by the matrix $[\mathcal{H}]$ whose the columns are the N_h sloshing-capillarity modes.

- C_U is the admissible space of the test functions δU, related to the structure occupying domain Ω_S (without dissipative terms and without given forces), coupled with the inviscid incompressible liquid occupying domain Ω_L, with the boundary condition $p = 0$ on Γ. We consider the subspace of C_U spanned by the elastic modes with added mass effects associated with the first N_u smallest positive eigenfrequencies and represented by the matrix $[\mathcal{U}]$ whose the columns are the N_u elastic modes with the added mass effects.

For solving the three generalized eigenvalue problems for large scale fluid-structure computational models with mid-power computers, we refer the reader to [63] in which all the details are given, for which the matrices of the generalized eigenvalue problems must be those introduced in Section 5.3.1, that is to say, using quadratic finite elements.

The reduced-order computational model of order (N_p, N_h, N_u) is obtained by projecting Eq. (29) on the subspace spanned by $([\mathcal{P}], [\mathcal{H}], [\mathcal{U}])$ and is written, for all $t \geq 0$, as

$$\mathbf{P}^{N_p,N_h,N_u}(t) = [\mathcal{P}]\,\mathbf{q}_p(t) \quad , \quad \mathbf{H}^{N_p,N_h,N_u}(t) = [\mathcal{H}]\,\mathbf{q}_h(t) \quad , \quad \mathbf{U}^{N_p,N_h,N_u}(t) = [\mathcal{U}]\,\mathbf{q}_u(t)\,, \tag{32}$$

$$[\mathcal{A}_{\rm FSI}]\,\mathbf{q}(t) = \mathcal{F}(t)\,, \tag{33}$$

in which $\mathbf{q}(t) = (\mathbf{q}_p(t), \mathbf{q}_h(t), \mathbf{q}_u(t))$.

6. Numerical application

This numerical application is designed to quantify the effects of the second term in the right-hand side of the new boundary equation defined by Eq. (23). This term has to be considered for taking into account the elasticity of the structure in the vicinity of the triple contact line. In Eq. (28) of the matrix system, this term corresponds to $-[C_{h\mathbf{u}}]^T\,\mathbf{H}(t)$. As we have mentioned in Section 1, the elasticity of the structure in the neighborhood of the triple line is usually approximated by a rigid moving wall. Based on the developments presented in this paper, the numerical application shows the role played by the elasticity in the neighborhood of this triple line.

6.1. Fluid-structure system: geometry, mechanical properties, boundary conditions, and finite element mesh

This application has been designed in order that the coupling between the elastic structure and the compressible fluid be only *via* the triple line.

(i) The considered system is a small elastic cup (cylindrical elastic wall with a bottom elastic plate), whose dimensions are given in the Figure 2 (left), containing a liquid for which the contact angle with the vertical elastic wall (cylindrical wall) is greater than 90° (non-wetting liquid). The liquid is in contact with the structure, only on the bottom of the cup and on the triple line, which is common to the vertical wall. Five contact angles are considered, $\theta \in \{143°, 152°, 161°, 169°, 177°\}$, which leads us to a modification of the curvature of the free surface especially at the triple line location, Figure 2 (right). It can be seen that the smaller the contact angle, the greater the local curvature of the surface at the triple line. Table 1 reports the local curvature $< K_\Gamma >$ of the free surface at the triple line as a function of the contact angle.

(ii) The elastic structure is homogeneous and isotropic: Young modulus $E = 50\,N.m^{-2}$, Poisson coefficient $\nu = 0.25$, mass density $\rho_S = 7900\,Kg.m^{-3}$, and damping rate 5×10^{-5}. The

	θ_1	θ_2	θ_3	θ_4	θ_5
$< K_\Gamma >$	408	332	315	252	93

Table 1: Curvature $< K_\Gamma >$ of the free surface at the triple line with respect to the considered contact angles θ_i, $i = 1, \ldots, 5$.

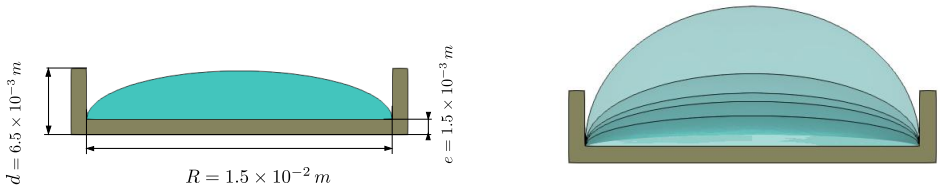

Figure 2: Left figure: Dimension of the fluid-structure system. Right figure: cross-section for the different contact angles θ.

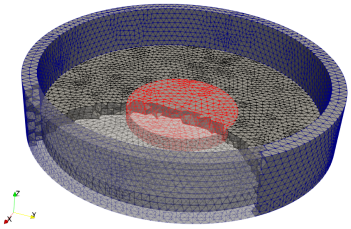

Figure 3: Boundary conditions and finite element mesh of the fluid-structure systems.

parameters of the acoustic fluid are: sound velocity $c_0 = 0.08\, m.s^{-1}$ and mass density $\rho_0 = 1000\, Kg.m^{-3}$. The parameters of the free surface are: surface tension coefficient $\sigma_\Gamma = 0.0728$, and gravity intensity $g = 9.81\, m.s^{-2}$.

(iii) The boundary conditions applied to the structure are defined in order to avoid the energy transmission from the structural excitation (which are radial forces applied to the vertical elastic cylindrical wall) to the liquid by the contact surface Γ_L. The configuration is designed for obtaining an energy transmission that is done only through the triple line. A portion of the bottom of the cup, located on a centered disk with a radius of $6 \times 10^{-3}\, m$ (part of the mesh colored red in Figure 3) is fixed in all three directions to prevent rigid body motions of the elastic structure. The nodes located in the rest of the cup bottom (black-color nodes in Figure 3) are locked along the vertical direction $\mathbf{e}_3$. This boundary condition prevents vertical displacements of the elastic structure on Γ_L, which means that $\mathbf{n} \cdot \mathbf{u} = 0$ on Γ_L (that implies that $[C_{pu}]$ matrix is removed from Eq. (28)). The nodes located in the rest of the structure (blue-color nodes in Figure 3) are left free. These boundary conditions ensure that the transmission of the excitation energy from the structure to the liquid is only done via the triple line.

(iv) The finite element model of the fluid-structure system is constructed using quadratic 3D tetrahedral finite elements with 10 nodes for the structure and for the acoustic liquid (see

Figure 3). The free surface of the liquid is meshed using quadratic 2D finite elements with 6 nodes and the triple line is meshed using 1D finite elements with 3 nodes, with quadratic interpolation functions. The dimension n_u of $\mathbf{U}$ is 37 014. The dimension n_p and n_h of $\mathbf{P}$ and $\mathbf{H}$ depends on the contact angle and are respectively, 7 068, 8 488, 9 227, 10 301, and 16 464 for n_p, and 2 269, 2 445, 2 541, 2 541, and 3 625 for n_h.

6.2. Eigenfrequency characterization

Table 2 presents the first eigenfrequencies of the coupled fluid-structure system corresponding to the three generalized eigenvalue problems defined in Section 5.4 for which the computational model is defined in Section 6.1-(iv). Note that a large number of eigenmodes will be used for computing the responses (see Section 6.5). The eigenfrequencies of the structure, of the liquid, and of the free surface are interlaced, which strongly induces coupling resonances in the dynamical responses of the system.

Contact angle	Sloshing-capillarity eigenfrequencies (in Hz)								
θ_1	2.82	4.61	6.51	6.61	8.52	9.93	10.89	13.31	13.42
θ_2	3.29	5.33	7.42	7.47	9.72	10.89	12.28	14.29	14.95
θ_3	3.56	5.75	7.82	8.01	10.35	11.24	13.05	14.58	14.71
θ_4	3.79	6.05	8.01	8.35	10.71	11.14	12.70	13.47	14.22
θ_5	3.58	5.58	6.61	7.67	8.37	8.82	9.97	11.15	12.01
Contact angle	Acoustic eigenfrequencies (in Hz)								
θ_1	8.35	9.26	10.7	10.26	11.09	11.26	12.00	12.25	12.35
θ_2	5.94	6.88	7.81	7.94	8.75	8.99	9.68	10.02	10.14
θ_3	5.18	6.14	7.08	7.24	8.04	8.31	8.97	9.36	9.49
θ_4	4.11	5.11	6.10	6.28	7.07	7.41	8.04	8.51	8.65
θ_5	2.84	3.97	5.03	5.22	5.87	6.07	6.35	6.96	7.08
Contact angle	Elastic eigenfrequencies with added mass effects (in Hz)								
$\{\theta_1, \theta_2, \theta_3, \theta_4, \theta_5\}$	2.97	4.08	5.84	6.56	6.63	7.37	7.79	8.92	9.08

Table 2: Table of the first 9 sloshing-capillarity eigenfrequencies of the free surface, acoustic eigenfrequencies of the liquid, and elastic eigenfrequencies with added mass effects of the structure (in Hz).

6.3. Quantities of interest

The results of the numerical simulations are observed by different quantities of interest defined on certain observation points. These interest quantities are chosen in order to visualize a global behavior of the fluid-structure system towards matrix $[C_{hu}]^T$. The interest quantities are defined for each part of the system as follows.

- For the structural displacement, the quantity of interest, dB^U, is defined as the spatial averaging of all the nodes. Let $\mathbf{U}_{\mathbf{x}_i^u}(t)$ be the vector in $\mathbb{R}^3$ of the 3 displacement dofs of node $\mathbf{x}_i^u$, which is constructed from $\mathbf{U}(t)$ (with values in $\mathbb{R}^{n_u}$). Let $\omega \mapsto \widehat{\mathbf{U}}_{\mathbf{x}_i^u}(2\pi\nu)$ be the Fourier transform of $t \mapsto \mathbf{U}_{\mathbf{x}_i^u}(t)$, the quantity of interest $dB^U(2\pi\nu)$ is defined by,

$$dB^U(2\pi\nu) = \frac{1}{n_u/3} \sum_{i=1}^{n_u/3} 20 \log_{10}(\| \widehat{\mathbf{U}}_{\mathbf{x}_i^u}(2\pi\nu) \|_{\mathbb{C}^3}) \quad , \tag{34}$$

- For the pressure in the acoustic liquid, the quantity of interest dB^P is defined by

$$dB^P(2\pi\nu) = \frac{1}{n_p}\sum_{i=1}^{n_p} 20\log_{10}(\,|\widehat{P}_i(2\pi\nu)|\,) \quad . \tag{35}$$

- For the free-surface elevation, the quantity of interest dB^H is defined by

$$dB^H(2\pi\nu) = \frac{1}{n_h}\sum_{i=1}^{n_h} 20\log_{10}(\,|\widehat{H}_i(2\pi\nu)|\,) \quad . \tag{36}$$

6.4. Definition of the external excitation of the system and of time integration parameters

The external forces applied to the elastic structure are radial forces defined hereinafter. We consider the sector of the cylindrical elastic wall defined by the polar angle $[-\pi/16\,,\,\pi/16]$. Let n_{exci} be the number of nodes belonging to this sector and located on the external surface of the cylindrical wall. A radial force is applied to each one of these nodes with an intensity equal to $1/n_{\text{exci}}$. These radial forces are represented by the time depending vector $\mathbf{F}_u(t)$

$$\mathbf{F}_u(t) = \alpha\, g(t)\, \mathbf{F} \quad , \tag{37}$$

in which the vector $\mathbf{F}$ is time independent and is such that $\|\mathbf{F}\| = 1$. In Eq. (37), α is the intensity coefficient taken as $\alpha = 5\times10^{-8}$ and $g(t)$ is the time function of the dynamical excitation, whose Fourier transform is constant in the frequency band of excitation, $\mathbb{B}_e = [\nu_{min}\,,\,\nu_{max}]\,Hz$, with $\nu_{min} = 1\,Hz$ and $\nu_{max} = 10\,Hz$. Time function g and its Fourier transform $\widehat{g}$ are written as,

$$g(t) = 2\,\frac{\sin(\pi\Delta\nu\, t)}{\pi\, t}\,\cos(2\pi\, s\,\Delta\nu\, t) \qquad , \qquad \widehat{g}(2\pi\nu) = \mathbb{1}_{\mathbb{B}_e\bigcup\underline{\mathbb{B}}_e}(\nu) \quad , \tag{38}$$

in which $\underline{\mathbb{B}}_e = [-\nu_{\max}\,,\,-\nu_{\min}]$, $\Delta\nu = \nu_{max} - \nu_{min}$ and $s = (\nu_{max} + \nu_{min})/(2\Delta\nu)$. In Eq. (38), one can see that $\widehat{g}(2\pi\nu) = 1$ if $\nu \in \mathbb{B}_e$ and 0 if $\nu \in \mathbb{R}^+\backslash\mathbb{B}_e$. The dynamical responses of the system are computed in the time domain. The Fourier transform of the time responses allows for obtaining the responses in the frequency domain over chosen frequency band of analysis $\mathbb{B}_a = [0\,,\,40]\,Hz$. The computation is carried out on a truncated time domain $[t_{ini},\, t_{ini} + T]$ with $t_{ini} = -66.67\,s$ and $T = 1\,469.32\,s$. Note that the sloshing-capillarity resonances are very weakly damped and consequently, require a long simulation time T before returning to equilibrium position. The sampling frequency and the number of time steps are chosen as $\nu_e = 80\,Hz$ and $N_t = 122\,880$.

6.5. Convergence of the reduced-order model

The linear reduced-order model used for the simulations requires a convergence analysis with respect to the size of the projection basis (see Section 5.4). Since the dynamical reference solution cannot be computed for such large-scale and long-time computational model, it is assumed that the convergence is reached when the response is no longer sensitive to parameters N_p, N_h or N_u. In the following, $\mathbf{X}$ denotes either $\mathbf{P}$, $\mathbf{H}$, or $\mathbf{U}$. The quantity of interest $dB^X(2\pi\nu)$ is rewritten as $dB^X(2\pi\nu; N_p, N_h, N_u)$ for indicating its dependency with respect to the modal truncation order N_p, N_h, and N_u. We choose to normalize the convergence function

with respect to the values $\overline{N}_p = 200$, $\overline{N}_h = 250$, and $\overline{N}_u = 100$. The convergence function $(N_p, N_h, N_u) \mapsto \mathrm{Conv}_X(N_p, N_h, N_u)$ is defined by,

$$\mathrm{Conv}_X(N_p, N_h, N_u) = \left\{ \frac{\displaystyle\int_{\mathbb{B}_a} dB^X(2\pi\nu; N_p, N_h, N_u)^2 \, d\nu}{\displaystyle\int_{\mathbb{B}_a} dB^X(2\pi\nu; \overline{N}_p, \overline{N}_h, \overline{N}_u)^2 \, d\nu} \right\}^{1/2} . \tag{39}$$

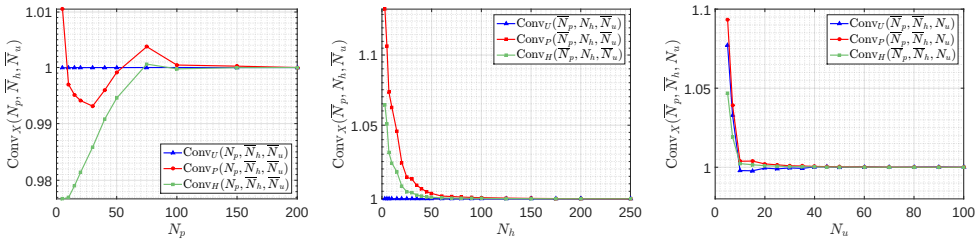

Figure 4: Graphs of the convergence of the solutions obtained in terms of **P**, **H**, and **U** at the observation points with respect to N_p (left figure), to N_h (middle figure), and to N_u (right figure).The vertical axis is in log scale.

Three convergence analyses are then performed with respect to N_p, to N_h, and to N_u. Figure 4 displays the graphs of

$$N_p \mapsto \mathrm{Conv}_X(N_p, \overline{N}_h, \overline{N}_u) \quad \text{for} \quad \mathbf{X} = \{\mathbf{P}, \mathbf{H}, \mathbf{U}\} \tag{40}$$

$$N_h \mapsto \mathrm{Conv}_X(\overline{N}_p, N_h, \overline{N}_u) \quad \text{for} \quad \mathbf{X} = \{\mathbf{P}, \mathbf{H}, \mathbf{U}\} \tag{41}$$

$$N_u \mapsto \mathrm{Conv}_X(\overline{N}_p, \overline{N}_h, N_u) \quad \text{for} \quad \mathbf{X} = \{\mathbf{P}, \mathbf{H}, \mathbf{U}\} \tag{42}$$

This convergence analyses yield the following optimal order of the ROM: $N_p = 100$, $N_h = 80$, and $N_u = 50$, which are used in the following calculations.

6.6. Quantification of the influence of $[C_{hu}]^T$ with respect to θ

In order to quantify the influence of the coupling matrix $[C_{hu}]^T$, two cases are considered. The first one, the coupling matrix $[C_{hu}]^T$ is kept in Eq. (28) (case of an elastic structure in the neighborhood of the triple line); the numerical results are presented in blue-dashed line in Figures 6 to 8. In the second one, the coupling matrix $[C_{hu}]^T$ is removed in Eq. (28) (case of a rigid structure in the neighborhood of the triple line); the numerical results are displayed in red-solid line in Figures 6 to 8. Figures 6, 7, and 8 respectively display the graphs of $\nu \mapsto dB^U(2\pi\nu)$, $\nu \mapsto dB^P(2\pi\nu)$, and $\nu \mapsto dB^H(2\pi\nu)$, for the five contact angles θ_i, $i = 1, \ldots, 5$. The results show that the coupling matrix $[C_{hu}]^T$ has a major influence on the dynamical response of the fluid-structure system. This influence can be seen on the graphs of dB^U (in Figure 6) for which some resonances appear on the frequency response, which do not occur when $[C_{hu}]^T$ is removed. In fact, one can see that the resonances in the frequency response dB^U without $[C_{hu}]^T$ correspond to structural eigenfrequencies (see Table 2). However, the resonances that occur in the frequency response dB^U with $[C_{hu}]^T$ are highly shifted, due to the coupling matrix $[C_{hu}]^T$.

This phenomenon is clearly seen for contact angle θ_1, for which two resonances appear in the neighborhood of the structural resonance located at 4.08 Hz. A resonance also appears in the graph of dB^U, for all the contact angles, located between 1.17 Hz and 1.58 Hz. This resonance is the first sloshing resonance that is shifted due to the coupling with a resonance of the elastic structure. The results show that the influence of $[C_{hu}]^T$ tends to decrease as the contact angle increases. In addition, the influence of $[C_{hu}]^T$ increases as the local curvature of the free surface increases. A possible explanation for this increasing influence of $[C_{hu}]^T$, which is inversely proportional to θ, is the increasing of the gap between c_h and d_h as θ increases, as shown in Figure 5. In this figure, one can notice that the difference between c_h and d_h is greater when the contact angle is small. In addition, we see that the term d_h becomes more important than the term c_h when moving towards small angles.

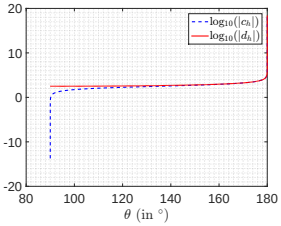

Figure 5: Graphs of $\theta \mapsto \log_{10}(|c_h|)$ (in blue solid line) and $\theta \mapsto \log_{10}(|d_h|)$ (in red solid line), which display the values of c_h and d_h for the curvature $< K_\Gamma >= 315$.

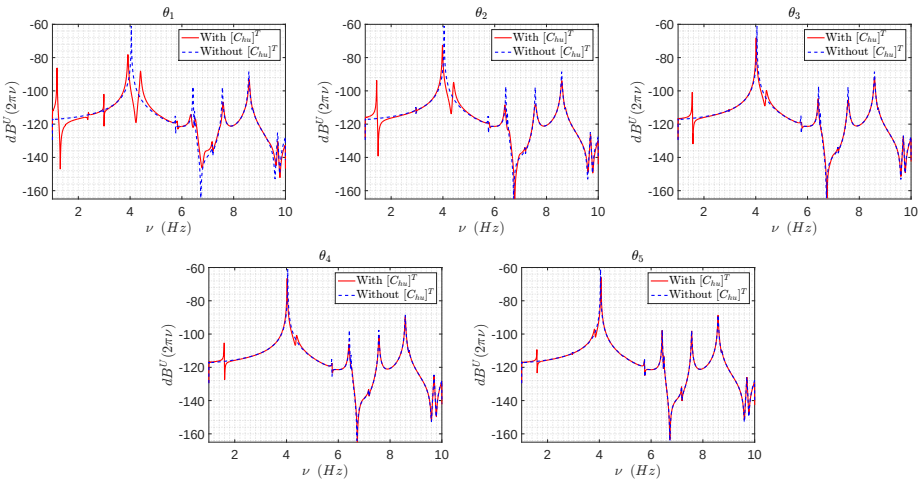

Figure 6: Graphs of $\nu \mapsto dB^U(2\pi\nu)$ for the contact angle $\theta_1 = 143°$ (top left), for the contact angle $\theta_2 = 152°$ (top middle), for the contact angle $\theta_3 = 161°$ (top right), for the contact angle $\theta_4 = 169°$ (down left), and for the contact angle $\theta_5 = 177°$ (down right).

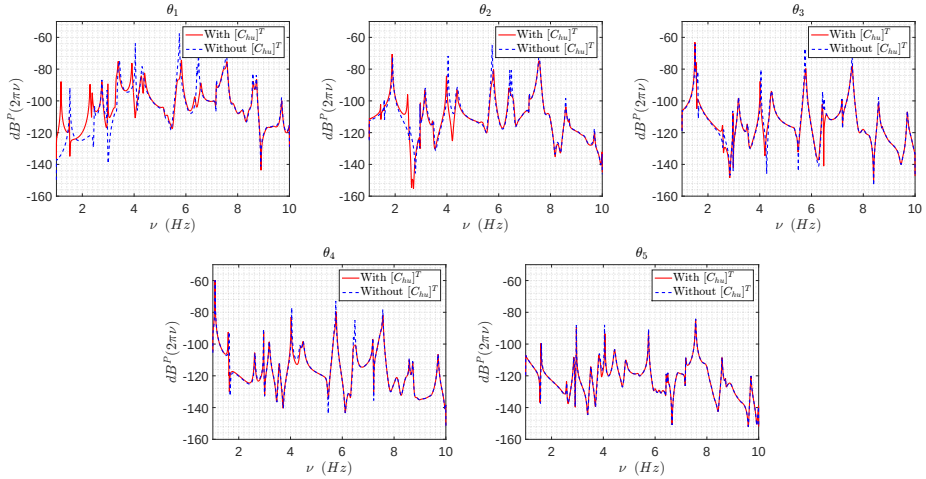

Figure 7: Graphs of $\nu \mapsto dB^P(2\pi\nu)$ for the contact angle $\theta_1 = 143°$ (top left), for the contact angle $\theta_2 = 152°$ (top middle), for the contact angle $\theta_3 = 161°$ (top right), for the contact angle $\theta_4 = 169°$ (down left), and for the contact angle $\theta_5 = 177°$ (down right).

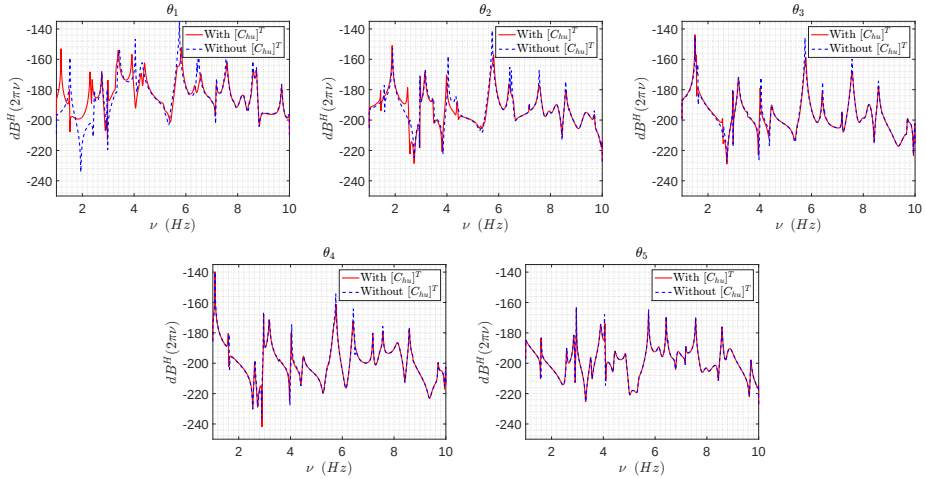

Figure 8: Graphs of $\nu \mapsto dB^H(2\pi\nu)$ for the contact angle $\theta_1 = 143°$ (top left), for the contact angle $\theta_2 = 152°$ (top middle), for the contact angle $\theta_3 = 161°$ (top right), for the contact angle $\theta_4 = 169°$ (down left), and for the contact angle $\theta_5 = 177°$ (down right).

7. Conclusion

In this paper and in the context of linear dynamics, we have quantified the effects of the 3D elasticity of a structure in the neighborhood of the triple contact line in presence of a 3D acoustic fluid with sloshing and surface tension effects. The functional analysis of the weak formulation of the 3D boundary value problem with the new boundary condition on the triple contact line

shows that quadratic finite elements have to be used for constructing the computational model. While the structure is generally considered as rigid in this neighborhood, the proposed novel formulation shows the importance of the elasticity. For this purpose a full numerical analysis has been presented using a purposely designed fluid-structure system in which the boundary conditions applied to the structure are defined in order to avoid the energy transmission from the structural excitation to the liquid by the liquid-structure interface but to have only an energy transmission by the triple contact line. It should be noted that most of the works consider that the structure is totally not deformable (rigid tank) or consider a locally undeformable structure in the neighborhood of the triple contact line. The numerical results that have been presented show that the influence of elasticity tends to decrease as the contact angle increases. In addition, this influence increases as the local curvature of the free surface increases. A possible explanation for this increasing influence, which is inversely proportional to the contact angle, is the increasing of the gap between parameters c_h and d_h as the contact angle increases.

References

[1] Abramson HN. *The dynamical behaviour of liquids in moving containers*. NASA publication SP-106 . 1966.

[2] Moiseyev NN, Rumyantsev VV. *Dynamic Stability of Bodies Containing Fluid*. Springer Verlag, New York . 1968.

[3] Morand H, Ohayon R. *Fluid Structure Interaction*. John Wiley & Sons, New York . 1995.

[4] Dodge FT. *The New Dynamic Behavior of Liquids in Moving Containers*. Southwest Research Institute, San Antonio, Texas . 2000.

[5] Ibrahim RA. *Liquid Sloshing Dynamics: Theory and Applications*. Cambridge University Press, Cambridge . 2005.

[6] Faltinsen OM, Timokha AN. *Sloshing*. 577. Cambridge University Press Cambridge . 2009.

[7] Chowdhury P. Fluid finite elements for added-mass calculations. *International Shipbuilding Progress* 1972; 19(217): 302–309. http://dx.doi.org/10.3233/ISP-1972-1921703 doi: 10.3233/ISP-1972-1921703

[8] Amabili M, Paidoussis MP, Lakis AA. Vibrations of partially filled cylindrical tanks with ring-stiffeners and flexible bottom. *Journal of Sound and Vibration* 1998; 213(2): 259–299. http://dx.doi.org/doi.org/10.1006/jsvi.1997.1481 doi: doi.org/10.1006/jsvi.1997.1481

[9] Zienkiewicz OC, Taylor RL, Zhu JZ. *The Finite Element Method: its Basis and Fundamentals*. Elsevier . 2005.

[10] Farhat C, Chiu EKY, Amsallem D, Schotté JS, Ohayon R. Modeling of fuel sloshing and its physical effects on flutter. *AIAA journal* 2013; 51(9): 2252–2265. http://dx.doi.org/10.2514/1.J052299 doi: 10.2514/1.J052299

[11] Bermúdez A, Rodríguez R, Santamarina D. Finite element computation of sloshing modes in containers with elastic baffle plates. *International Journal for Numerical Methods in Engineering* 2003; 56(3): 447–467. http://dx.doi.org/10.1002/nme.578 doi: 10.1002/nme.578

[12] González JA, Park KC, Lee I, Felippa C, Ohayon R. Partitioned vibration analysis of internal fluid-structure interaction problems. *International Journal for Numerical Methods in Engineering* 2012; 92(3): 268–300. http://dx.doi.org/10.1002/nme.4336 doi: 10.1002/nme.4336

[13] Schotté JS, Ohayon R. Incompressible hydroelastic vibrations: finite element modelling of the elastogravity operator. *Computers & structures* 2005; 83(2-3): 209–219. http://dx.doi.org/10.1016/j.compstruc.2004.03.084 doi: 10.1016/j.compstruc.2004.03.084

[14] Ohayon R, Soize C. *Structural Acoustics and Vibration: Mechanical Models, Variational Formulations and Discretization*. Elsevier . 1997.

[15] Van Brummelen E. Added mass effects of compressible and incompressible flows in fluid-structure interaction. *Journal of Applied mechanics* 2009; 76(2): 021206. http://dx.doi.org/10.1115/1.3059565 doi: 10.1115/1.3059565

[16] Bazilevs Y, Takizawa K, Tezduyar TE. *Computational Fluid-Structure Interaction: Methods and Applications*. John Wiley & Sons . 2013.

[17] Lighthill J. *Waves in Fluids*. MA: Cambridge University Press . 1978.

[18] Andrianarison O, Ohayon R. Reduced models for modal analysis of fluid-structure systems taking into account compressibility and gravity effects. *Computer Methods in Applied Mechanics and Engineering* 2006; 195: 5656–5672. http://dx.doi.org/10.1016/j.cma.2005.11.013 doi: 10.1016/j.cma.2005.11.013

[19] Chu WH, Kana DD. A theory for nonlinear transverse vibrations of a partially filled elastic tank. *AIAA Journal* 1967; 5(10): 1828–1835. http://dx.doi.org/10.2514/3.4312 doi: 10.2514/3.4312

[20] Dias F, Kharif C. Nonlinear gravity and capillary-gravity waves. *Annual Review of Fluid Mechanics* 1999; 31(1): 301–346. http://dx.doi.org/10.1146/annurev.fluid.31.1.301 doi: 10.1146/annurev.fluid.31.1.301

[21] Ohayon R, Soize C. Nonlinear model reduction for computational vibration analysis of structures with weak geometrical nonlinearity coupled with linear acoustic liquids in the presence of linear sloshing and capillarity. *Computers & Fluids* 2016; 141: 82–89. http://dx.doi.org/10.1016/j.compfluid.2016.03.032 doi: 10.1016/j.compfluid.2016.03.032

[22] Akkaoui Q, Capiez-Lernout E, Soize C, Ohayon R. Revisiting the experiment of a free-surface resonance of a liquid in a vibration tank using a nonlinear fluid–structure computational model. *Journal of Fluids and Structures* 2019; 85: 149–164. http://dx.doi.org/10.1016/j.jfluidstructs.2019.01.005 doi: 10.1016/j.jfluidstructs.2019.01.005

[23] Abramson HN, Kana DD, Lindholm US. An experimental study of liquid instability in a vibrating elastic tank. *Journal of Spacecraft and Rockets* 1966; 3(8): 1183–1188.

[24] Abramson HN, Kana DD. Some experimental studies of the dynamic stability of thin shells containing liquid. *Academy of Science USSR* 1970; Anniversary volume in honor of V. Novozhilov.

[25] Myshkis AD, Babskii VG, Kopachevskii ND, Slobozhanin LA, Tyuptsov AD. *Low-Gravity Fluid Mechanics*. Springer-Verlag Berlin Heidelberg New York . 1987.

[26] Bonn D, Eggers J, Indekeu J, Meunier J, Rolley E. Wetting and spreading. *Reviews of Modern Physics* 2009; 81(2): 739-805. http://dx.doi.org/10.1103/RevModPhys.81.739 doi: 10.1103/RevModPhys.81.739

[27] Landau L, Lifchitz E. *Fluid Mechanics*. Elsevier, Amsterdam . 2011.

[28] De Gennes PG, Brochard-Wyart F, Quéré D. *Capillarity and Wetting Phenomena: Drops, Bubbles, Pearls, Waves*. Springer Science & Business Media . 2013.

[29] Finn R. On the equations of capillarity. *Journal of Mathematical Fluid Mechanics* 2001; 3(2): 139-151. http://dx.doi.org/10.1007/PL00000966 doi: 10.1007/PL00000966

[30] Ruschak KJ. A method for incorporating free boundaries with surface tension in finite element fluid-flow simulators. *International Journal for Numerical Methods in Engineering* 1980; 15(5): 639–648. http://dx.doi.org/10.1002/nme.1620150502 doi: 10.1002/nme.1620150502

[31] Christodoulou KN, Scriven LE. The fluid mechanics of slide coating. *Journal of Fluid Mechanics* 1989; 208: 321–354. http://dx.doi.org/10.1017/S0022112089002855 doi: 10.1017/S0022112089002855

[32] Bellet M. Implementation of surface tension with wall adhesion effects in a three-dimensional finite element model for fluid flow. *Communications in Numerical Methods in Engineering* 2001; 17(8): 563–579. http://dx.doi.org/10.1002/cnm.430 doi: 10.1002/cnm.430

[33] Dettmer W, Saksono PH, Perić D. On a finite element formulation for incompressible Newtonian fluid flows on moving domains in the presence of surface tension. *Communications in Numerical Methods in Engineering* 2003; 19(9): 659–668. http://dx.doi.org/10.1002/cnm.628 doi: 10.1002/cnm.628

[34] Dettmer W, Perić D. A computational framework for free surface fluid flows accounting for surface tension. *Computer Methods in Applied Mechanics and Engineering* 2006; 195(23-24): 3038–3071. http://dx.doi.org/10.1016/j.cma.2004.07.057 doi: 10.1016/j.cma.2004.07.057

[35] Saksono PH, Perić D. On finite element modelling of surface tension. Variational formulation and applications–Part I: Quasistatic problems. *Computational Mechanics* 2006; 38(3): 265–281.

[36] Saksono PH, Perić D. On finite element modelling of surface tension: Variational formulation and applications–Part II: Dynamic problems. *Computational Mechanics* 2006; 38(3): 251–263. http://dx.doi.org/10.1007/s00466-005-0745-7 doi: 10.1007/s00466-005-0745-7

[37] Van Brummelen E, Shokrpour-Roudbari M, Van Zwieten G. Elasto-capillarity simulations based on the Navier–Stokes–Cahn–Hilliard equations. In: *Advances in Computational Fluid-Structure Interaction and Flow Simulation* 2016: 451–462, Springer.

[38] Nezit P. Hydrodynamics-Gravity waves with surface tension. *Journal de Mecanique* 1977; 16: 39–66.

[39] Finn R, Luli GK. On the capillary problem for compressible fluids. *Journal of Mathematical Fluid Mechanics* 2007; 9(1): 87-103. http://dx.doi.org/0.1007/s00021-005-0203-5 doi: 0.1007/s00021-005-0203-5

[40] Leblond JB, El Sayed HA, Bergheau JM. On the incorporation of surface tension in finite-element calculations. *Comptes Rendus Mécanique* 2013; 341(11-12): 770–775. http://dx.doi.org/10.1016/j.crme.2013.10.004 doi: 10.1016/j.crme.2013.10.004

[41] Concus P, Finn R. On the behavior of a capillary surface in a wedge. *Proceedings of the National Academy of Sciences of the United States of America* 1969; 63(2): 292. http://dx.doi.org/10.1073/pnas.63.2.292 doi: 10.1073/pnas.63.2.292

[42] Finn R. The contact angle in capillarity. *Physics of Fluids* 2006; 18(4): 047102. http://dx.doi.org/10.1063/1.2185655 doi: 10.1063/1.2185655

[43] Das S, Marchand A, Andreotti B, Snoeijer JH. Elastic deformation due to tangential capillary forces. *Physics of Fluids* 2011; 23(7): 072006. http://dx.doi.org/10.1063/1.3615640 doi: 10.1063/1.3615640

[44] Dussan V EB. On the spreading of liquids on solid surfaces: static and dynamic contact lines. *Annual Review of Fluid Mechanics* 1979; 11(1): 371–400. http://dx.doi.org/10.1146/annurev.fl.11.010179.002103 doi: 10.1146/annurev.fl.11.010179.002103

[45] Pukhnachev V, Solonnikov V. On the problem of dynamic contact angle. *Journal of Applied Mathematics*

and Mechanics 1983; 46(6): 771–779. http://dx.doi.org/10.1016/0021-8928(82)90059-4 doi: 10.1016/0021-8928(82)90059-4

[46] Dussan V EB, Ramé E, Garoff S. On identifying the appropriate boundary conditions at a moving contact line: an experimental investigation. *Journal of Fluid Mechanics* 1991; 230: 97–116. http://dx.doi.org/10.1017/S0022112091000721 doi: 10.1017/S0022112091000721

[47] Shikhmurzaev YD. Moving contact lines in liquid/liquid/solid systems. *Journal of Fluid Mechanics* 1997; 334: 211–249. http://dx.doi.org/10.1017/S0022112096004569 doi: 10.1017/S0022112096004569

[48] Kidambi R, Shankar P. The effects of the contact angle on sloshing in containers. *Proceedings of the Royal Society of London. Series A: Mathematical, Physical and Engineering Sciences* 2004; 460(2048): 2251–2267. http://dx.doi.org/10.1098/rspa.2004.1281 doi: 10.1098/rspa.2004.1281

[49] Thompson PA, Robbins MO. Simulations of contact-line motion: slip and the dynamic contact angle. *Physical Review Letters* 1989; 63(7): 766. http://dx.doi.org/10.1103/PhysRevLett.63.766 doi: 10.1103/PhysRevLett.63.766

[50] Keller JB, Merchant GJ. Flexural rigidity of a liquid surface. *Journal of Statistical Physics* 1991; 63(5-6): 1039–1051. http://dx.doi.org/10.1007/BF01029998 doi: 10.1007/BF01029998

[51] Starov VM. Equilibrium and hysteresis contact angles. *Advances in Colloid and Interface Science* 1992; 39: 147–173. http://dx.doi.org/10.1016/0001-8686(92)80059-7 doi: 10.1016/0001-8686(92)80059-7

[52] White LR. The contact angle on an elastic substrate. 1. The role of disjoining pressure in the surface mechanics. *Journal of Colloid and Interface Science* 2003; 258(1): 82–96. http://dx.doi.org/10.1016/S0021-9797(02)00090-5 doi: 10.1016/S0021-9797(02)00090-5

[53] Ostrach S. Low-gravity fluid flows. *Annual Review of Fluid Mechanics* 1982; 14(1): 313–345. http://dx.doi.org/10.1146/annurev.fl.14.010182.001525 doi: 10.1146/annurev.fl.14.010182.001525

[54] Bauer HF, Eidel W. Linear liquid oscillations in cylindrical container under zero-gravity. *Applied Microgravity Technology* 1990; 2: 212–220.

[55] Cocciaro B, Faetti S, Nobili M. Capillarity effects on surface gravity waves in a cylindrical container: wetting boundary conditions. *Journal of Fluid Mechanics* 1991; 231: 325–343. http://dx.doi.org/10.1017/S0022112091003415 doi: 10.1017/S0022112091003415

[56] Henderson DM, Miles J. Surface-wave damping in a circular cylinder with a fixed contact line. *Journal of Fluid Mechanics* 1994; 275: 285–299. http://dx.doi.org/10.1017/S0022112094002363 doi: 10.1017/S0022112094002363

[57] El-Kamali M, Schotté JS, Ohayon R. Three-dimensional modal analysis of sloshing under surface tension. *International Journal for Numerical Methods in Fluids* 2011; 65(1-3): 87-105. http://dx.doi.org/10.1002/fld.2457 doi: 10.1002/fld.2457

[58] Ohayon R, Soize C. Vibration of structures containing compressible liquids with surface tension and sloshing effects. Reduced-order model. *Computational Mechanics* 2015; 55(6): 1071-1078. http://dx.doi.org/10.1007/s00466-014-1091-4 doi: 10.1007/s00466-014-1091-4

[59] Ohayon R, Soize C. *Advanced Computational Vibroacoustics: Reduced-Order Models and Uncertainty Quantification*. Cambridge University Press, New York . 2014.

[60] Lions JL, Magenes E. *Non-homogeneous Boundary Value Problems and Applications*. 1. Springer-Verlag . 1972.

[61] Douady A, Krée P. *Séminaire Douady-Krée 1965-1966: Espaces Vectoriels Topologiques et Distributions*. Université de Nice . 1966.

[62] Dautray R, Lions JL. *Mathematical Analysis and Numerical Methods for Science and Technology*. Springer Science & Business Media . 2013.

[63] Akkaoui Q, Capiez-Lernout E, Soize C, Ohayon R. Solving generalized eigenvalue problems for large scale fluid-structure computational models with mid-power computers. *Computers & Structures* 2018; 205: 45–54. http://dx.doi.org/10.1016/j.compstruc.2018.04.007 doi: 10.1016/j.compstruc.2018.04.007